LETTERS

Redox-mediated substrate recognition by Sdp1 defines a new group of tyrosine phosphatases

G. C. Fox[1]*†, M. Shafiq[1]*, D. C. Briggs[1], P. P. Knowles[1], M. Collister[4], M. J. Didmon[4], V. Makrantoni[5], R. J. Dickinson[4], S. Hanrahan[2], N. Totty[2], M. J. R. Stark[5], S. M. Keyse[4] & N. Q. McDonald[1,3]

Reactive oxygen species trigger cellular responses by activation of stress-responsive mitogen-activated protein kinase (MAPK) signalling pathways[1,2]. Reversal of MAPK activation requires the transcriptional induction of specialized cysteine-based phosphatases that mediate MAPK dephosphorylation[3]. Paradoxically, oxidative stresses generally inactivate cysteine-based phosphatases by thiol modification and thus could lead to sustained or uncontrolled MAPK activation[4,5]. Here we describe how the stress-inducible MAPK phosphatase, Sdp1, presents an unusual solution to this apparent paradox by acquiring enhanced catalytic activity under oxidative conditions. Structural and biochemical evidence reveals that Sdp1 employs an intramolecular disulphide bridge and an invariant histidine side chain to selectively recognize a tyrosine-phosphorylated MAPK substrate. Optimal activity critically requires the disulphide bridge, and thus, to the best of our knowledge, Sdp1 is the first example of a cysteine-dependent phosphatase that couples oxidative stress with substrate recognition. We show that Sdp1, and its paralogue Msg5, have similar properties and belong to a new group of phosphatases unique to yeast and fungal taxa.

MAPK phosphatases (MKPs) have a Cys-$(X)_5$-Arg catalytic motif and a conserved general acid Asp, both characteristic of cysteine-based phosphatases (CBPs)[6,7]. Most MKPs are dual-specific for phosphothreonine and phosphotyrosine, although phosphotyrosine-specific MKPs have also been identified[3,8,9]. Each can target and dephosphorylate phospho-residues within the MAPK activation loop thereby inhibiting MAPK activity[3]. MKPs are often transcriptionally induced following stimulation of their target MAPK as part of a negative feedback loop to attenuate MAPK signalling[3]. When the activating stimulus for a MAPK involves reactive oxygen species, this poses a conundrum as, like all CBPs, MKPs are potentially sensitive to oxidative inactivation[5,10]. Protective mechanisms have been described for CBPs that prevent irreversible oxidative damage to the catalytic cysteine, either through a sulphenyl-amide intermediate (PTP1B) or by formation of a reversible intramolecular disulphide bond with the catalytic cysteine (PTEN, CDC25, KAP, MKP-3)[5,11,12]. In each case the phosphatase is inactivated, albeit reversibly. In yeast, adaptation to oxidative stress is a necessary requisite for survival and multiple MAPKs are known to respond to oxidative stimuli, including Slt2/Mpk1 (refs 1, 13, 14). Moreover, strains lacking Slt2 are hypersensitive to oxidants[14–17]. We predicted that MKPs specific for Slt2, which are required to operate under oxidative conditions, may employ mechanisms to deal with this environmental stress. Slt2 forms part of a signalling cascade required to maintain cell wall integrity and can also respond to other stresses such as heat shock[18]. Regulation of Slt2 involves at least four distinct MKPs able to dephosphorylate Slt2 directly[13]. However, only the stress-dependent phosphatase Sdp1, induced by peroxide stimulus, is specific for Slt2 (refs 19, 20). We therefore investigated how Sdp1 is able to dephosphorylate a MAPK substrate under oxidative conditions.

In the presence of the reducing agent dithiothreitol (1 mM DTT) Sdp1 exhibited a relatively poor K_m (Michaelis constant) of 14.5 mM towards the chromogenic phosphatase substrate *para*-nitrophenyl phosphate (pNPP) (Fig. 1a). However, in the absence of reducing agents, Sdp1 has a K_m value of 0.6 mM, indicating a 24-fold enhanced affinity for pNPP substrate and therefore a much higher catalytic efficiency (Fig. 1a). The k_{cat} for pNPP remained approximately the same in the presence or absence of reducing agent. In marked contrast, the VHR phosphatase, typical of other CBPs, required reducing agents to maintain its reactive thiol in a reduced form (Fig. 1a).

Sdp1 has been shown to dephosphorylate both activated Slt2 and the closely related mammalian ERK2 MAPK[19,20]. Western blots using anti-phospho-specific antibodies showed that Sdp1 exclusively targets the phosphotyrosine residue of activated ERK2 known to be required for catalytic activity (Fig. 1b). Remarkably, the absence of reducing agent has a dramatic effect on the kinetics of phosphotyrosine dephosphorylation by Sdp1 (Fig. 1b). All ERK2 phosphotyrosine is hydrolysed within 10 min without DTT, whereas total hydrolysis is not achieved even after 2 h of incubation in the presence of 1 mM DTT (Fig. 1b). Both the dual-specificity MKP-3 and tyrosine-specific VHR phosphatases were able to dephosphorylate activated ERK2 fully under these conditions[21,22] (Fig. 1c). Thus, Sdp1 is the first reported cysteine-based phosphatase that is essentially inactivated by reducing agents.

Dual-specificity MKPs that use an amino-terminal non-catalytic domain in MAPK substrate recognition have been described[3], and therefore we assayed a truncated Sdp1 spanning approximately the core phosphatase domain (56–197; Fig. 1c). This protein exhibited no activity towards phospho-ERK2 with or without DTT, suggesting that critical residue(s) were missing (Fig. 1c). To identify the region of Sdp1 required for ERK2 dephosphorylation and optimal pNPP activity we performed a deletion analysis from the amino terminus and found that residues 46–55 were essential (Fig. 1d). Sdp1 has only three cysteine residues (Fig. 1c) and one of these, Cys 47, is within this region. Quantification of the number of free sulphydryl groups in Sdp1 using Ellman's reagent (DTNB) suggested only a single free sulphydryl group was available, which we presumed corresponded to the Cys 140 active site residue (Fig. 2a). A C140S active site mutant of Sdp1 exhibited no reactivity with DTNB indicating there were no available –SH groups, which is consistent with Cys 47 and Cys 142

[1]Structural Biology Laboratory and [2]Protein Analysis Laboratory, The London Research Institute, Cancer Research UK, 44 Lincoln's Inn Fields, London WC2A 3PX, UK. [3]School of Crystallography, Birkbeck College, Malet Street, London WC1E 7HX, UK. [4]Cancer Research UK, Stress Response Laboratory, Biomedical Research Centre, Ninewells Hospital, Dundee DD1 9SY, UK. [5]Division of Gene Regulation and Expression, College of Life Sciences, MSI/WTB Complex, University of Dundee, Dundee DD1 5EH, UK. †Present address: ESRF, 6 Rue Jules Horowitz, 38043 Grenoble, Cedex 9, France.
* These authors contributed equally to this work.

forming a disulphide bridge (Fig. 2a). To obtain direct evidence for an intramolecular Cys 47–Cys 142 disulphide bridge, we analysed a trypsin-digest of the Sdp1(C140S) mutant by matrix-assisted laser desorption/ionization–time of flight (MALDI-TOF) mass spectrometry (MS) (Fig. 2b and Supplementary material). A disulphide-linked peptide at mass/charge ratio (*m/z*) 2,475 was identified and further fragmented by MS/MS CID (collision-induced dissociation). This generated two sets of triplet signals corresponding to symmetric (*m/z* 1,226 and 1,251) and asymmetric cleavage of the disulphide bridge linking the peptides EFVPCSSLDVR (residues 43–53) and ILIHSQCGLSR (residues 136–146) (Fig. 2b and Supplementary Table 1). Conversely, a reduced and alkylated Sdp1(C140S) mutant showed no *m/z* 2,475 ion after trypsin digestion but showed the equivalent cysteine peptide ions modified by alkylation (Supplementary Table 1). As expected from our biochemical analysis C47S, C142S as well as the C47S/C142S double Sdp1 mutant were all catalytically inactive towards phospho-ERK2 and exhibited only minimal basal activity towards pNPP (Fig. 2c and d). Moreover, these low-activity Sdp1 cysteine mutants were now insensitive to the presence of reducing agents (Fig. 2d).

Intramolecular disulphide bond formation can result in increased migration of proteins analysed by non-reducing SDS–polyacrylamide

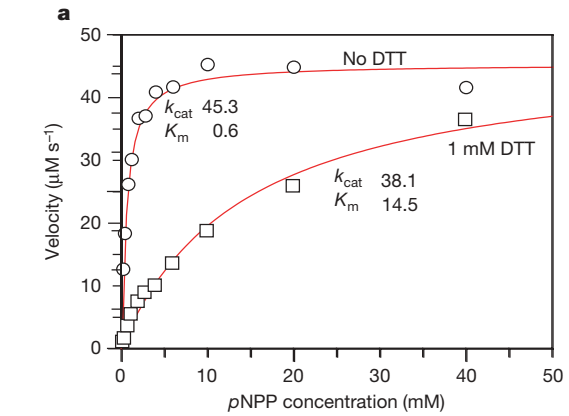

Protein	Kinetic constants (sec^{-1}) and (mM)	Catalytic efficiency
Sdp1(FL)	k_{cat} 49.2 ± 0.5 K_m 0.7 ± 0.03	70.3
Sdp1(FL) + DTT	k_{cat} 34.8 ± 0.5 K_m 12.5 ± 0.6	2.8
Sdp1	k_{cat} 45.3 ± 0.8 K_m 0.6 ± 0.05	75.5
Sdp1 + DTT	k_{cat} 38.1 ± 2.3 K_m 14.5 ± 1.8	2.6
VHR	k_{cat} 52.2 ± 0.7 K_m 32.0 ± 1.0	1.6
VHR + DTT	k_{cat} 117.0 ± 2.4 K_m 28.9 ± 1.4	4.0

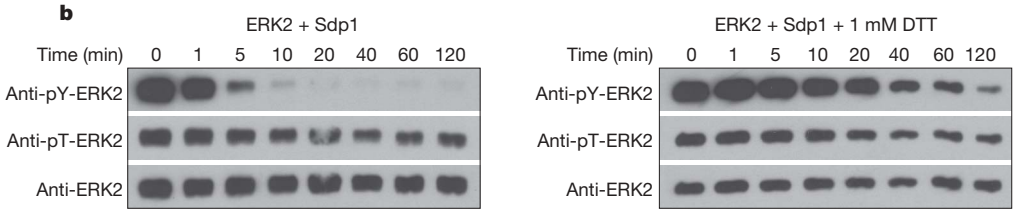

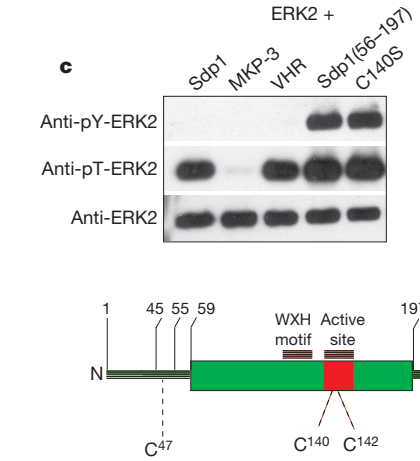

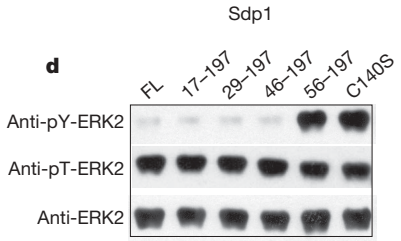

Protein	Kinetic constants (sec^{-1}) and (mM)	Catalytic efficiency
Sdp1	k_{cat} 44.6 ± 0.8 K_m 0.7 ± 0.13	63.7
Sdp1(29–197)	k_{cat} 44.1 ± 1.3 K_m 0.9 ± 0.1	49.0
Sdp1(46–197)	k_{cat} 31.9 ± 0.8 K_m 0.6 ± 0.07	53.2
Sdp1(56–197)	k_{cat} 11.5 ± 0.7 K_m 13.8 ± 1.8	0.8
C140S	Not detectable	None

Figure 1 | Sdp1 activity is sensitive to reducing agents. a, Effect of DTT on the Sdp1 kinetic constants for pNPP hydrolysis. Solid lines indicate fit to the Michaelis–Menten equation. Tabulated rate constants and s.e.m. for Sdp1 and VHR are also shown. Catalytic efficiency is defined as k_{cat}/K_m. Sdp1 is used to indicate a truncated form of Sdp1 (residues 17 to 197) used for structural and biochemical work as well as for the Sdp1 point mutants. Full-length Sdp1, indicated by Sdp1(FL), gave equivalent kinetic constants for both wild-type and mutant proteins. **b**, Time course of recombinant activated (diphosphorylated) ERK2 dephosphorylation by Sdp1 in the presence (right panel) or absence (left panel) of reducing agent, detected using phosphothreonine (pT) or phosphotyrosine (pY) specific antibodies by western blot analysis. **c**, Upper panel shows activated ERK2 dephosphorylation after a two-hour incubation with Sdp1 (no DTT) or the dual-specific DUSP6/MKP-3 and the tyrosine-specific VHR (both with 1 mM DTT). A truncated Sdp1 (residues 56–197) and a catalytically dead Sdp1(C140S) mutant were also tested without DTT. Lower panel shows a schematic for Sdp1, indicating the position of cysteine residues, and demarcates the catalytic CBP domain in green. **d**, Upper panel, activity of a series of N-terminal Sdp1 deletion mutants towards phospho-ERK2 by western blot, as previously described. Lower panel, same series of mutants and their activity towards pNPP.

a

Sample	Theoretical -SH	Measured -SH content
Sdp1	3	0.57 ± 0.04
Reduced Sdp1	3	3.11 ± 0.21
Sdp1 (C140S)	2	0.00
Reduced Sdp1 (C140S)	2	2.21 ± 0.10
BSA (17 disulphides)	35	0.57 ± 0.01
Glutathione	1	1.00 ± 0.02

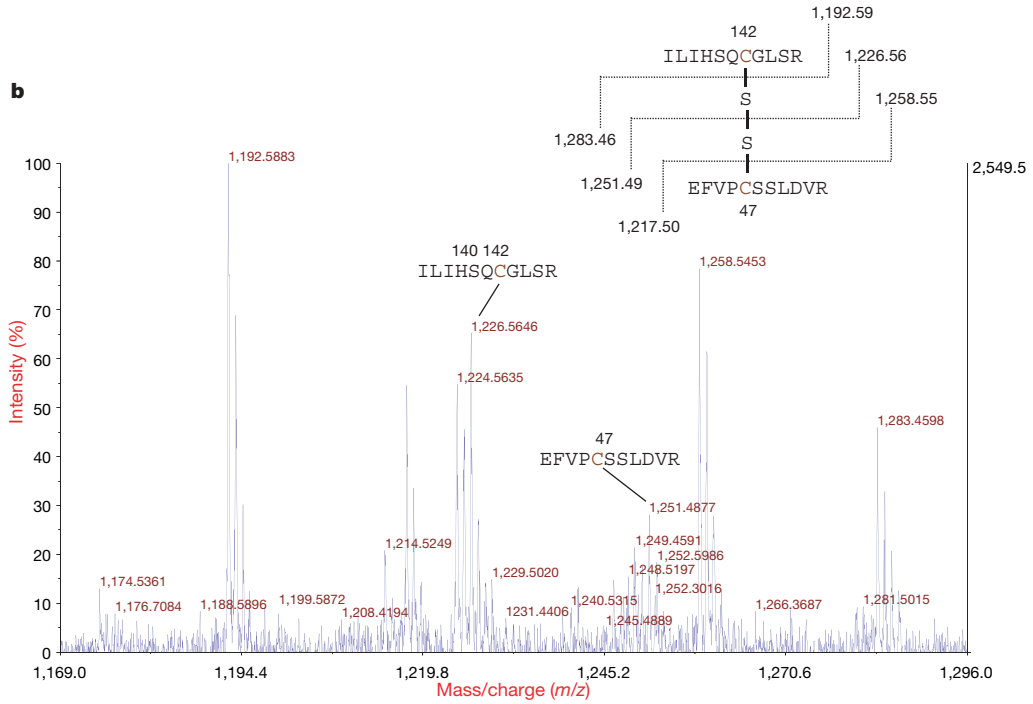

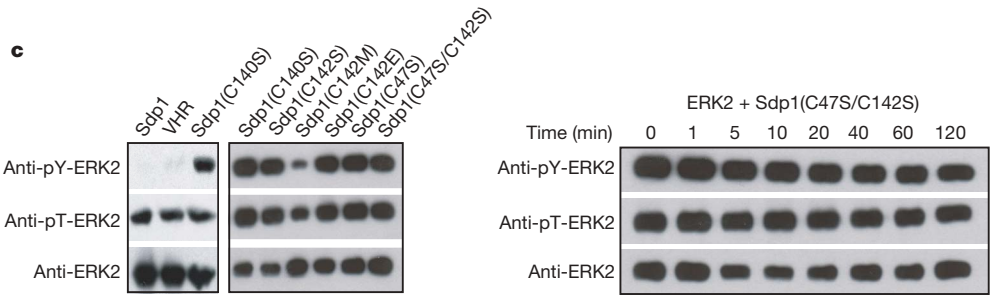

d

Protein	Kinetic constants (sec^{-1}) and (mM)		Catalytic efficiency
Sdp1	k_{cat}	45.7 ± 0.8	57.1
	K_m	0.8 ± 0.06	
Sdp1 + DTT	k_{cat}	38.1 ± 2.3	2.6
	K_m	14.5 ± 1.8	
C47S/ C142S	k_{cat}	25.0 ± 0.7	2.1
	K_m	12.0 ± 1.0	
C47S/C142S + DTT	k_{cat}	29.0 ± 2.4	2.1
	K_m	14.0 ± 1.4	

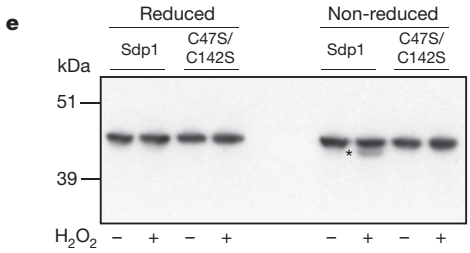

Figure 2 | Sdp1 activity requires an intramolecular Cys 47–Cys 142 disulphide bridge. **a**, Table of the free sulphydryl (-SH) content of wild type and various cysteine mutants of Sdp1 as measured by Ellman's reagent titration using glutathione and BSA as controls. **b**, MS/MS fragmentation spectrum of the Cys 47–Cys 142 disulphide-linked precursor ion at *m/z* 2,475. Inset, interpretation of the fragmentation. **c**, Activated ERK2 dephosphorylation by the Sdp1 cysteine point mutants (left panel) performed as described in the legend of Fig. 1c and a time course for the C47S/C142S double mutant (right panel). **d**, Kinetic rate constants for Sdp1 cysteine point mutants measured by pNPP hydrolysis. **e**, Analysis of the Sdp1 redox state *in vivo* by anti-Myc immunoblot. Sdp1 null yeast expressing either wild-type Myc–Sdp1 or Myc–Sdp1 C47S/C142S were subjected to heat shock at 39 °C for 45 min to induce Sdp1 expression and then either left untreated or exposed to H_2O_2 (0.4 mM) for 15 min. Protein extracts were then analysed by SDS–PAGE under non-reducing or reducing conditions, as indicated. The disulphide-containing Sdp1 protein with increased mobility is indicated by an asterisk.

gel electrophoresis (PAGE)[23]. To determine if the formation of an intramolecular disulphide bond within Sdp1 might be of physiological relevance, we have directly analysed the *in vivo* redox state of Sdp1 by SDS–PAGE and western blotting (Fig. 2e). As previously observed for the transcription factor Yap1, which forms an intramolecular disulphide bond when yeast cells are exposed to H_2O_2 (ref. 23), a proportion of the Sdp1 from H_2O_2-treated cells migrates more quickly than the protein from untreated cells under non-reducing conditions (lanes 5 and 6). However, this mobility shift was not detected after electrophoresis under reducing conditions (lanes 1 and 2). This shift is due to formation of an intramolecular disulphide, because the migration of Sdp1(C47S/C142S) was completely unaffected by exposure of yeast to H_2O_2 when analysed under non-reducing conditions (lanes 7 and 8). We also detect a distinct electrophoretic mobility shift when recombinant wild-type Sdp1 is analysed in the absence of DTT, which also depends on the integrity of Cys 47 and Cys 142, but not Cys 140 (see Supplementary Material and Supplementary Fig. 3).

To confirm our biochemical observations we determined the crystal structures of Sdp1 alone, bound to sulphate and phosphotyrosine as substrate mimetics (Fig. 3a). Superposition of the three molecules shows the equivalent general acid loop of CBPs in three discrete conformations corresponding to an open form with a 3_{10} helix, a partially closed form in the presence of sulphate in which the 3_{10} helix 'melts' and a fully closed state bound to phosphotyrosine (Fig. 3a, left panel). These changes reveal how the His 111 sidechain in the CBP acid loop moves into position only when a phosphotyrosine substrate occupies the active site. The structural changes are analogous to those observed for PTP1B and proposed as part of the activation mechanism for MKP-3, but involve a histidine rather than an aspartic acid[24,25].

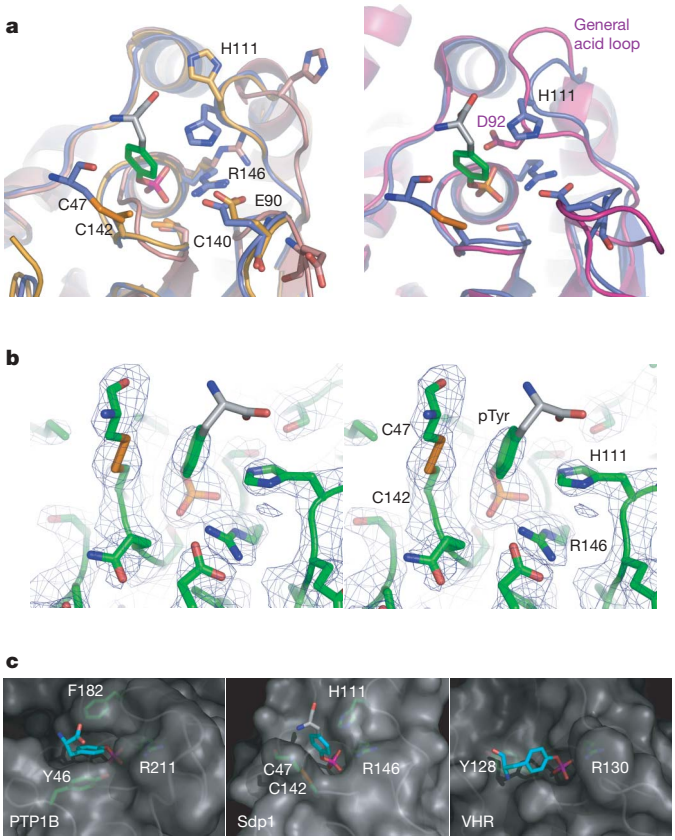

Figure 3 | Phosphotyrosine recognition by His 111 and the Cys 47–Cys 142 disulphide bridge. a, Left panel shows substrate-induced conformational changes in the Sdp1 active site. Apo (pink), sulphate- (gold) and phosphotyrosine-bound (blue) Sdp1. Right panel shows a superposition of Sdp (phosphotyrosine-bound) and VHR (magenta), indicating His 111 is structurally equivalent to aspartic acid 92 of VHR. **b**, Stereoview of a SIGMAA-weighted ($2F_o$–F_c) electron density map contoured at 1σ close to the Sdp1 active site, highlighting density for the His 111 side chain and Cys 47–Cys 142 disulphide bridge. The phosphotyrosine ring is shown in green and red, mainchain atoms for phosphotyrosine omitted from the refined model are shown in grey. **c**, Surface representation of the active sites of Sdp1, VHR and PTP1B with phosphotyrosine substrates, and equivalent phosphotyrosine contact residues, identified.

His 111 is structurally equivalent to the general acid aspartic acid residue of VHR (Fig. 3a, right panel). However, although it is required for ERK2 dephosphorylation it does not have a catalytic role (see Supplementary Material and Supplementary Fig. 2) and is likely to assist in phosphotyrosine recognition. His 111 is part of a loop motif Trp-X-His-X-Ser/Thr in which the Trp is buried and the Ser side chain stabilizes the loop conformation (Supplementary Fig. 1b). Sequence searches with the Trp-X-His-X-Ser/Thr and Cys-$(X)_5$-Arg motifs found matches exclusively within yeast and filamentous fungi genomes (Fig. 4a). We found two hits with these motifs in *Saccharomyces cerevisiae* corresponding to Sdp1 (YIL113W; *Saccharomyces* Genome Database at http://www.yeastgenome.org) and Msg5 (YNL053L). Both phosphatases are known to target Slt2 and their respective genes map to regions related by whole-genome duplication[19,26,27] (Fig. 4a). To test whether Msg5 is also sensitive to reducing agents, we assayed the activity of Msg5 towards pNPP and found that, like Sdp1, it exhibited a much poorer K_m in the presence of DTT than in its absence (Fig. 4b). Similarly, we found that mutation of the two cysteines C80S/C321S, analogous to the Sdp1 double cysteine mutant, eliminated the sensitivity to DTT (Fig. 4b). Thus, Sdp1 and Msg5 have equivalent catalytic properties.

Budding yeasts (hemi-ascomycetes) that phylogenetically branched off before the *S. cerevisiae* genome duplication, as well as filamentous fungi and fission yeast genomes, encode a single phosphatase bearing the Trp-X-His-X-Ser/Thr and C-$(X)_5$-Arg motifs (Fig. 4a). All budding yeast hits with these motifs have retained an equivalent cysteine to Cys 142 of Sdp1, suggesting that they too will be regulated in a similar manner to Sdp1 and Msg5 (Fig. 4a). The precise half-cysteine partner for Cys 142 cannot be reliably predicted in these cases owing to lack of sequence conservation and the presence of multiple cysteine residues in their respective N-terminal domains (data not shown). In contrast, matches to phosphatases encoded by filamentous fungi and fission yeast genomes lack an equivalent Cys 142, suggesting they may exhibit a different regulatory mechanism from Sdp1, Msg5 and budding yeast equivalents. For example, Pmp1 from fission yeast lacks a Cys 142 equivalent and requires the presence of DTT for activity (Fig. 4a and 4b). It has a methionine at this position (Fig. 4a), suggesting that this residue could functionally substitute for the intramolecular disulphide bridge. Consistent with this idea, we found that a C142M mutant Sdp1 retains some activity towards ERK2 but lost any sensitivity towards DTT (Fig. 2c and data not shown).

Our results establish a new group of MAPK phosphatases specific for yeast and fungal taxa that we propose should be classified as WH phosphatases because the Trp and His residues within the

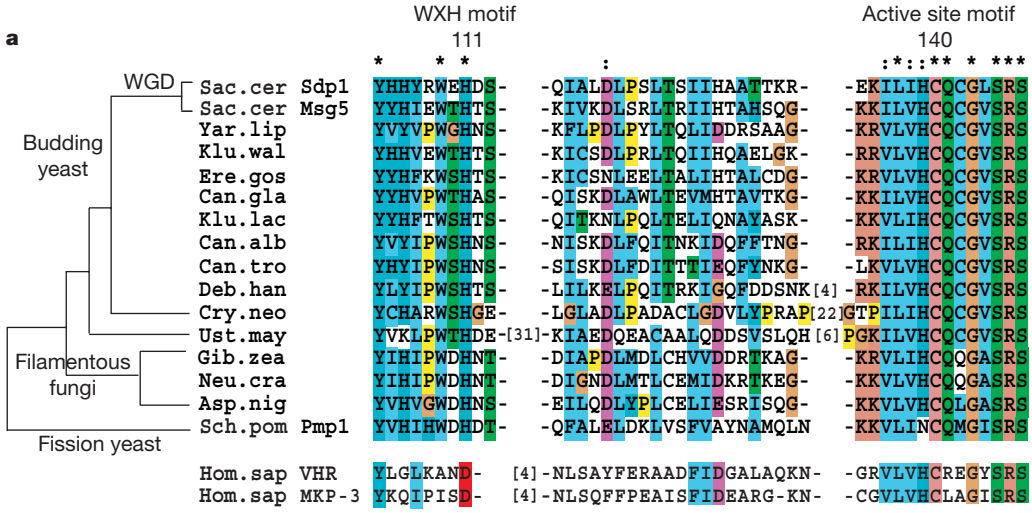

Figure 4 | Sdp1 and Msg5 are prototypic members of the WH phosphatase family. a, Sequence alignment of Sdp1 and related WH phosphatases close to their active site. Structurally equivalent sequences from MKP-3 and VHR are shown on the bottom for comparison. Selected organisms with a WH phosphatase are clustered according to consensus phylogeny indicating hemiascomycotina (budding yeasts), filamentous ascomycota (filamentous fungi) and representatives of basidiomycota (*Ustilago maydis*) and archiascomycotina (fission yeast) subphyla. Connectors are of arbitrary length. WGD, whole genome duplication. Sac cer, *Saccharomyces cerevisiae*; Sch pom, *Schizosaccharomyces pombe*; Yar lip, *Yarrowica lipolytica*; Klu wal, *Kluyveromyces waltii*; Ere gos, *Eremothecium gossypii*; Can gla, *Candida glabrata*; Klu lac, *Kluyveromyces lactis*; Can alb, *Candida albicans*; Can tro, *Candida tropicalis*; Deb han, *Debaryomyces hansenii*; Cry neo, *Cryptococcus neoformans*; Ust may, *Ustilago maydis*; Gib zea, *Gibberella zeae*; Neu cra, *Neurospora crassa*; Asp nig, *Aspergillus niger*; and Hom sap, *Homo sapiens*. **b**, Msg5 activity towards pNPP shows similar sensitivity to reducing agents as Sdp1. Equivalent conditions to those described in Fig. 1a were used with or without 1 mM DTT. Pmp1, which lacks a predicted intramolecular disulphide, does not exhibit reductant sensitivity. **c**, Model for the activation of Sdp1 under oxidative conditions leading to Slt2 dephosphorylation. *SDP1* synthesis is controlled by the Msn2/4 transcription factor (reviewed in ref. 13).

Trp-X-His-X-Ser/Thr motif are absolutely conserved in all cases (Fig. 4a). These phosphatases were not previously recognized as being closely related owing to sequence alignment errors close to the Trp-X-His-X-Ser/Thr motif (see DSPc/PF00782 Pfam entry at http://www.sanger.ac.uk/Software/Pfam). In light of our findings, published biochemical experiments may need to be re-evaluated for Sdp1 and Msg5. They also raise the question as to whether there are functionally analogous phosphatases in higher eukaryotes operating under oxidative conditions that would inactivate MAPKs[28]. Phosphatase oxidation has emerged as an important control mechanism to regulate these enzymes negatively in response to cell surface receptor activation[4,10]. Our observations identify an unprecedented mechanism for protein tyrosine phosphatase activation through a disulphide bridge that does not involve the catalytic cysteine (Fig. 4c). Once redox equilibrium is restored inside the cell, Sdp1 activation would most probably be reversed by reduction of this disulphide bond. Slt2 and Sdp1 synthesis is also responsive to heat shock and this stress may increase oxidative metabolism leading to higher levels of endogenous reactive oxygen species that in turn activate Sdp1. Yeast employ a variety of mechanisms to recognize and adapt to oxidative stress that frequently involve the reversible formation of disulphide bonds[29,30]. The existence of an analogous mechanism for Sdp1 shows that yeast have evolved a strategy to overcome the intrinsic limitation of using thiol-based phosphatases to counter and reverse oxidative-activation of a stress responsive MAPK.

METHODS

All proteins used in this study were produced in *Escherichia coli* and purified using an affinity tag. Crystals were grown using the hanging-drop vapour diffusion method. Diffraction data were collected at the European Synchrotron Radiation Facility at Grenoble and the Synchrotron Radiation Source at Daresbury. The apo/sulphate crystal structure was solved by molecular replacement using a composite search model of MKP-3 catalytic domain (Protein Data Bank, 1MKP) and VHR structures (PDB, 1VHR). The Sdp1(C140S)–phosphotyrosine structure was solved using the Sdp1/sulphate coordinates. Enzymatic assays were performed as previously described using either pNPP or recombinant diphosphorylated ERK2 as a substrate[20]. The free

sulphydryl content was measured using Ellman's reagent (Pierce Chemicals) according to the manufacturer's instructions. Tryptic digests of the Sdp1(C140S) mutant were analysed by mass spectrometry using an Applied Biosystems 4700 Proteomics Analyser. *In vivo* experiments used an Sdp1 null yeast strain transformed with a low copy number plasmid expressing a Myc-tagged Sdp1 or Sdp1 mutants driven by the endogenous *SDP1* promoter. After induction of Sdp1, yeast were exposed to H_2O_2, pelleted and lysed to produce protein extracts for analysis as described previously[23].

Received 13 February; accepted 3 April 2007.
Published online 9 May 2007.

1. Ikner, A. & Shiozaki, K. Yeast signaling pathways in the oxidative stress response. *Mutat. Res.* **569,** 13–27 (2005).
2. Chang, L. & Karin, M. Mammalian MAP kinase signalling cascades. *Nature* **410,** 37–40 (2001).
3. Keyse, S. M. Protein phosphatases and the regulation of mitogen-activated protein kinase signalling. *Curr. Opin. Cell Biol.* **12,** 186–192 (2000).
4. Tonks, N. K. Redox redux: revisiting PTPs and the control of cell signaling. *Cell* **121,** 667–670 (2005).
5. Salmeen, A. & Barford, D. Functions and mechanisms of redox regulation of cysteine-based phosphatases. *Antioxid. Redox Signal.* **7,** 560–577 (2005).
6. Barford, D., Das, A. K. & Egloff, M. P. The structure and mechanism of protein phosphatases: insights into catalysis and regulation. *Annu. Rev. Biophys. Biomol. Struct.* **27,** 133–164 (1998).
7. Alonso, A. *et al.* Protein tyrosine phosphatases in the human genome. *Cell* **117,** 699–711 (2004).
8. Pulido, R., Zuniga, A. & Ullrich, A. PTP-SL and STEP protein tyrosine phosphatases regulate the activation of the extracellular signal-regulated kinases ERK1 and ERK2 by association through a kinase interaction motif. *EMBO J.* **17,** 7337–7350 (1998).
9. Mattison, C. P., Spencer, S. S., Kresge, K. A., Lee, J. & Ota, I. M. Differential regulation of the cell wall integrity mitogen-activated protein kinase pathway in budding yeast by the protein tyrosine phosphatases Ptp2 and Ptp3. *Mol. Cell. Biol.* **19,** 7651–7660 (1999).
10. Rhee, S. G., Bae, Y. S., Lee, S. R. & Kwon, J. Hydrogen peroxide: a key messenger that modulates protein phosphorylation through cysteine oxidation. *Sci. STKE* **1,** doi:10.1126/stke.2000.53.pe1 (2000).
11. Salmeen, A. *et al.* Redox regulation of protein tyrosine phosphatase 1B involves a sulphenyl-amide intermediate. *Nature* **423,** 769–773 (2003).
12. Seth, D. & Rudolph, J. Redox regulation of MAP kinase phosphatase 3. *Biochemistry.* 45,–8476–8487 (2006).
13. Martin, H., Flandez, M., Nombela, C. & Molina, M. Protein phosphatases in MAPK signalling: we keep learning from yeast. *Mol. Microbiol.* **58,** 6–16 (2005).
14. Staleva, L., Hall, A. & Orlow, S. J. Oxidative stress activates *FUS1* and *RLM1* transcription in the yeast *Saccharomyces cerevisiae* in an oxidant-dependent manner. *Mol. Biol. Cell* **15,** 5574–5582 (2004).
15. Alic, N., Higgins, V. J., Pichova, A., Breitenbach, M. & Dawes, I. W. Lipid hydroperoxides activate the mitogen-activated protein kinase Mpk1p in *Saccharomyces cerevisiae. J. Biol. Chem.* **278,** 41849–41855 (2003).
16. Vilella, F., Herrero, E., Torres, J. & de la Torre-Ruiz, M. A. Pkc1 and the upstream elements of the cell integrity pathway in *Saccharomyces cerevisiae*, Rom2 and Mtl1, are required for cellular responses to oxidative stress. *J. Biol. Chem.* **280,** 9149–9159 (2005).
17. Krasley, E., Cooper, K. F., Mallory, M. J., Dunbrack, R. & Strich, R. Regulation of the oxidative stress response through Slt2p-dependent destruction of cyclin C in *Saccharomyces cerevisiae. Genetics* **172,** 1477–1486 (2006).
18. Levin, D. E. Cell wall integrity signaling in *Saccharomyces cerevisiae. Microbiol. Mol. Biol. Rev.* **69,** 262–291 (2005).
19. Hahn, J. S. & Thiele, D. J. Regulation of the *Saccharomyces cerevisiae* Slt2 kinase pathway by the stress-inducible Sdp1 dual specificity phosphatase. *J. Biol. Chem.* **277,** 21278–21284 (2002).
20. Collister, M. *et al.* YIL113w encodes a functional dual-specificity protein phosphatase which specifically interacts with and inactivates the Slt2/Mpk1p MAP kinase in *S. cerevisiae. FEBS Lett.* **527,** 186–192 (2002).
21. Groom, L. A., Sneddon, A. A., Alessi, D. R., Dowd, S. & Keyse, S. M. Differential regulation of the MAP, SAP and RK/p38 kinases by Pyst1, a novel cytosolic dual-specificity phosphatase. *EMBO J.* **15,** 3621–3632 (1996).
22. Todd, J. L., Tanner, K. G. & Denu, J. M. Extracellular regulated kinases (ERK) 1 and ERK2 are authentic substrates for the dual-specificity protein-tyrosine phosphatase VHR. A novel role in down-regulating the ERK pathway. *J. Biol. Chem.* **274,** 13271–13280 (1999).
23. Delauney, A., Pflieger, D., Barrault, M. B., Vinh, J. & Toledano, M. B. A thiol peroxidase is an H_2O_2 receptor and redox-transducer in gene activation. *Cell* **111,** 471–481 (2002).
24. Jia, Z., Barford, D., Flint, A. J. & Tonks, N. K. Structural basis for phosphotyrosine peptide recognition by protein tyrosine phosphatase 1B. *Science* **268,** 1754–1758 (1995).
25. Stewart, A. E., Dowd, S., Keyse, S. M. & McDonald, N. Q. Crystal structure of the MAPK phosphatase Pyst1 catalytic domain and implications for regulated activation. *Nature Struct. Biol.* **6,** 174–181 (1999).
26. Kellis, M., Birren, B. W. & Lander, E. S. Proof and evolutionary analysis of ancient genome duplication in the yeast *Saccharomyces cerevisiae. Nature* **428,** 617–624 (2004).
27. Flandez, M., Cosano, I. C., Nombela, C., Martin, H. & Molina, M. Reciprocal regulation between Slt2 MAPK and isoforms of Msg5 dual-specificity protein phosphatase modulates the yeast cell integrity pathway. *J. Biol. Chem.* **279,** 11027–11034 (2004).
28. Kamata, H. *et al.* Reactive oxygen species promote TNFα-induced death and sustained JNK activation by inhibiting MAP kinase phosphatases. *Cell* **120,** 649–661 (2005).
29. Barford, D. The role of cysteine residues as redox-sensitive regulatory switches. *Curr. Opin. Struct. Biol.* **14,** 679–686 (2004).
30. Veal, E. A. *et al.* A 2-Cys peroxiredoxin regulates peroxide-induced oxidation and activation of a stress-activated MAP kinase. *Mol. Cell* **15,** 129–139 (2004).

Supplementary Information is linked to the online version of the paper at www.nature.com/nature.

Acknowledgements G.C.F. was supported by a studentship from GlaxoSmithKline. N.Q.M. and S.M.K. are funded by CR-UK. M.J.R.S. is supported by BBSRC. We thank M. Toledano for experimental advice, T. Kuno for the Pmp1 plasmid and M. Way for critical comments on the manuscript. We also thank M. Cobb for the gift of the ERKpTpY expression vector, D. Thiele and J.-S. Hahn for yeast strains and Sdp1 expression plasmids, and A. Stewart, S. Tilley and J. Denu for assistance with early experiments.

Author Contributions G.C.F. and N.Q.M. determined the apo and sulphate-bound structures. M.S. determined the phosphotyrosine structure and carried out pNPP and ERK2 assays and blots. D.C.B. and N.Q.M. refined the structures. P.P.K. measured the free -SH content and reproduced all kinetic experiments. S.M.K. and M.J.R.S. designed the *in vivo* assays. M.C, M.J.D, V.M., and R.J.D. carried out *in vivo* assays using Myc-tagged Sdp1 proteins. S.H. and N.T carried out the mass spectrometry. S.M.K. and N.Q.M planned the project and designed the experiments. N.Q.M., S.M.K. and D.C.B. wrote the paper.

Author Information Reprints and permissions information is available at www.nature.com/reprints. Coordinates have been deposited at the PDB with accession codes 2j16 (apo/sulphate-bound Sdp1) and 2j17 (phosphotyrosine–Sdp1 complex). The authors declare no competing financial interests. Correspondence and requests for materials should be addressed to N.Q.M. (neil.mcdonald@cancer.org.uk).